Noname manuscript No.
(will be inserted by the editor)

Channel Noise Effects on Neural Synchronization

Brenton Maisel · **Sadique Sheik** · **Katja Lindenberg**

arXiv:1704.02351v1 [q-bio.NC] 7 Apr 2017

Received: date / Accepted: date

Abstract Synchronization in neural networks is strongly tied to the implementation of cognitive processes, but abnormal neuronal synchronization has been linked to a number of brain disorders such as epilepsy and schizophrenia. Here we examine the effects of channel noise on the synchronization of small Hodgkin-Huxley neuronal networks. The principal feature of a Hodgkin-Huxley neuron is the existence of protein channels that transition between open and closed states with voltage dependent rate constants. The Hodgkin-Huxley model assumes infinitely many channels, so fluctuations in the number of open channels do not affect the voltage. However, real neurons have finitely many channels which lead to fluctuations in the membrane voltage and modify the timing of the spikes, which may in turn lead to large changes in the degree of synchronization. We demonstrate that under mild conditions, neurons in the network reach a steady state synchronization level that depends only on the number of neurons in the network. The channel noise only affects the time it takes to reach the steady state synchronization level.

Keywords Synchronization · Hodgkin-Huxley · Channel Noise · Neural Network

B. Maisel
Department of Chemistry and Biochemistry, University of California San Diego, La Jolla, California 92093-0340, USA
E-mail: bmaisel@ucsd.edu

S. Sheik
BioCircuits Institute, University of California San Diego, La Jolla, California 92093-0340, USA

K. Lindenberg
Department of Chemistry and Biochemistry, University of California San Diego, La Jolla, California 92093-0340, USA

1 Introduction

The human brain is estimated to contain over 100 billion neurons, with each neuron connected to approximately 10^4 other neurons. [13] Neurons influence each other through excitatory and inhibitory synaptic connections, and as a result, neurons in a network are rhythmically activated and inhibited through their synaptic connectivity [6]. Most of the brain's cognitive functions are based on synchronized interactions of a large number of neurons distributed across different brain areas [35,11,8,29,30]. For example, when monkeys learn categorical information (e.g., how to distinguish between groups of negative and positive objects), experiments have shown increased neural synchronization between the prefrontal cortex and the striatum [3].

In addition to the cognitive roles of synchronization, abnormal synchronization has been linked to a number of brain disorders such as epilepsy, schizophrenia, Alzheimer's disease, and Parkinson's disease[1,18,32]. For example, epilepsy has commonly been associated with excessive synchronization of neural populations [24,32] whereas schizophrenia has been associated with impaired neural synchronization [31,33]. In combination with cognitive function, it is clear that the balance between synchronized and asynchronized neural oscillations plays a pivotal role in healthy brain activity.

In order to model neuronal synchronization, many studies have focused on networks of Hodgkin-Huxley neurons. One defining property of the Hodgkin-Huxley neuron model that allows for action potential generation is the existence of sodium and potassium channels which transition between open and closed states with voltage-dependent rate constants. Each channel is composed of four gates: the sodium channel is composed of three activating gates (known as type m gates) and one inactivating gate (known as a type h gate), and the potassium channel is composed of four activating

gates of type n. At rest, the activating gates are closed and the inactivating gate is open, but as a neuron receives synaptic input from other neurons, the membrane voltage rises, causing the activating gates to open, which starts the depolarization of the membrane potential. When the voltage is high enough, the sodium inactivating gate closes while the potassium gates remain open, which repolarizes the membrane potential. The dynamics of the n gates and m gates are similar, but the n gate dynamics evolve on a slower time scale [34].

However, while the Hodgkin-Huxley model assumes that there are infinitely many channels so that fluctuations in the number of open channels remain undetected, real neurons have only finitely many channels and hence experience intrinsic noise through the stochastic opening and closing of sodium and potassium protein channels in the neural membrane. This stochasticity leads to fluctuations in the membrane potential which can alter spike timing of neurons. We refer to this stochasticity as channel noise, and its role in neural synchronization is the focus of our paper.

In this study, we investigate the synchronization of a small network of noisy Hodgkin-Huxley neurons. We select this neuron for study because of its close connection to biological reality and its ability to reproduce almost all single-neuron propeties [21,5,23]. A channel can only conduct when it is considered open, and a channel is considered open when all the gates within the channel are open. The most direct approach to modeling the opening and closing of channels is referred to as the Markov Chain model. In the Markov Chain Model, each of N channels of a particular type functions as a Markov process, transitioning between open and closed states with voltage-dependent rate constant, independently of other same-type channels. At each time step, one then determines the fraction of open channels of a particular type. These fractions are then used explicitly in the Hodgkin-Huxley voltage equation to model fluctuations in the membrane voltage due to channel noise. However, simulating such a Markov Chain is computationally exhaustive as one must compute the state of each channel individually, which takes a long time when dealing with thousands of channels. In order to account for perturbations in the Hodgkin-Huxley model, some studies have added an external perturbation to the Hodgkin-Huxley equations to assess the role of noise in synchronization [4,25,28]. This method, however, lacks justification that it accurately models the stochastic opening and closing of channels.

As an alternative, we use a set of stochastic differential equations developed by Fox and Lu which approximates the behavior of the Markov Chain model [10]. The stochastic equations of Fox and Lu do not modify the deterministic structure of the Hodgkin-Huxley equations, and they include stochastic perturbations which account for the opening and closing of channels. We refer to these stochastic perturbations as channel noise to be consistent with previous literature [14,15]. Results of numerical simulations of this model agree remarkably well with the dynamical behavior predicted by the Markov Chain model of the channel states [14,15]. To summarize, we have discussed three models: the original Hodgkin-Huxley model of a neuron, the Markov Chain model which models stochasticity in the channels transitioning randomly between open and closed states, and the Fox and Lu model which we will use due to its highly accurate approximation of the Markov Chain model but with a much faster computational time. Our goal is to understand how channel noise affects the synchronicity of neurons in a network, and we will use the Fox and Lu model to do so.

Our paper is organized as follows: In Sec. 2, we present a mathematical description of the stochastic Hodgkin-Huxley neuron with a synaptic connectivity term. Then in Sec. 3, we analyze how channel noise affects the synchronization of a network of neurons, and derive a formula to estimate the degree of synchronization based upon the size of the neural network. We then conclude with some closing remarks.

2 Model

One of the most important models in computational neuroscience is the Hodgkin-Huxley neuronal model of a squid axon [20,21]. The deterministic dynamics of the Hodgkin-Huxley model are given by the following set of differential equations:

$$\begin{aligned} C\dot{V} &= I_{inj}(t) + I_{syn}(t) - \bar{g}_{Na} m^3 h (V - E_{Na}) \\ &\quad - \bar{g}_K n^4 (V - E_K) - \bar{g}_L (V - E_L) \\ \dot{n} &= \alpha_n(V)(1-n) - \beta_n(V) n \\ \dot{m} &= \alpha_m(V)(1-m) - \beta_m(V) m \\ \dot{h} &= \alpha_h(V)(1-h) - \beta_h(V) h \end{aligned} \tag{1}$$

where:

$$\begin{aligned} \alpha_n(V) &= \frac{0.01V + 0.55}{1 - \exp[-0.1V - 5.5]} \\ \beta_n(V) &= 0.125 \exp[-(V+65)/80] \\ \alpha_m(V) &= \frac{0.1V + 4}{1 - \exp[-0.1V - 4]} \\ \beta_m(V) &= 4 \exp[-(V+65)/18] \\ \alpha_h(V) &= 0.07 \exp[-(V+65)/20] \\ \beta_h(V) &= \frac{1}{1 + \exp[-0.1V - 3.5]} \end{aligned}$$

The values of the parameters along with definitions are found in Table 1 [21].

Table 1 Parameter values used for simulation of the Hodgkin-Huxley model.

Parameter	Definition	Value
C	membrane capacitance	$1\mu F/cm^2$
E_{Na}	sodium reversal potential	$50mV$
E_K	potassium reversal potential	$-77mV$
E_L	leak reversal potential	$-54.4mV$
$\bar{g}_{Na}$	maximal sodium conductance	$120mS/cm^2$
$\bar{g}_K$	maximal potassium conductance	$36mS/cm^2$
$\bar{g}_L$	maximal leak conductance	$0.3mS/cm^2$

The fundamental feature of the Hodgkin-Huxley neuron model is the presence of channels in the neuron which conduct electricity when the channel is in an open state. The Hodgkin-Huxley model assumes that there are infinitely many channels, and consequently, fluctuations in the fraction of open channels due to their stochastic opening and closing do not have an effect on the membrane voltage. On the other hand, real neurons have only finitely many channels, so membrane voltage is affected by fluctuations in the number of open channels. The most direct method of modeling the Markov Chain model is to take a population of ion channels and a small time step dt, and then calculate the probability that each channel flipped from its current state to another state during the time interval. Although this method works, it is extraordinarily slow when the number of ion channels is large [27]. To counter this problem, we use the Fox and Lu system size expansion which is a stochastic differential equation that replicates the behavior of the Markov Chain model with high accuracy and less computational exhaustion [10,14,15]. The Fox and Lu system size expansion is given by the following set of stochastic differential equations:

$$\begin{aligned} C\dot{V} &= I_{inj}(t) + I_{syn}(t) - \bar{g}_{Na} y_{31}(V - E_{Na}) \\ &\quad - \bar{g}_K x_4 (V - E_K) - \bar{g}_L (V - E_L) \\ \dot{\mathbf{x}} &= A_K(V)\mathbf{x} + \frac{1}{\sqrt{N_K}} S_K(V,\mathbf{x})\xi_K \\ \dot{\mathbf{y}} &= A_{Na}(V)\mathbf{y} + \frac{1}{\sqrt{N_{Na}}} S_{Na}(V,\mathbf{y})\xi_{Na} \end{aligned} \tag{2}$$

$$A_K = \begin{bmatrix} -4\alpha_n & \beta_n & 0 & 0 & 0 \\ 4\alpha_n & -3\alpha_n - \beta_n & 2\beta_n & 0 & 0 \\ 0 & 3\alpha_n & -2\alpha_n - 2\beta_n & 3\beta_n & 0 \\ 0 & 0 & 2\alpha_n & -\alpha_n - 3\beta_n & 4\beta_n \\ 0 & 0 & 0 & \alpha_n & -4\beta_n \end{bmatrix}$$

$$A_{Na} = \begin{bmatrix} -3\alpha_m & \beta_m & 0 & 0 & \beta_h & 0 & 0 & 0 \\ 3\alpha_m & -2\alpha_m - \beta_m - \alpha_h & 2\beta_m & 0 & 0 & \beta_h & 0 & 0 \\ 0 & 2\alpha_m & -\alpha_m - 2\beta_m - \alpha_h & 3\beta_m & 0 & 0 & \beta_h & 0 \\ 0 & 0 & \alpha_m & -3\beta_m - \alpha_h & 0 & 0 & 0 & \beta_h \\ \alpha_h & 0 & 0 & 0 & -3\alpha_m - \beta_h & \beta_m & 0 & 0 \\ 0 & \alpha_h & 0 & 0 & 3\alpha_m & -2\alpha_m - \beta_m - \beta_h & 2\beta_m & 0 \\ 0 & 0 & \alpha_h & 0 & 0 & 2\alpha_m & -\alpha_m - 2\beta_m - \beta_h & 3\beta_m \\ 0 & 0 & 0 & \alpha_h & 0 & 0 & \alpha_m & -3\beta_m - \beta_h \end{bmatrix}$$

S_K and S_{Na} are the square root matrices of the following diffusion matrices:

$$D_K = \begin{bmatrix} 4\alpha_n x_0 + \beta_n x_1 & -4\alpha_n x_0 - \beta_n x_1 & 0 & 0 & 0 \\ -4\alpha_n x_0 - \beta_n x_1 & 4\alpha_n x_0 + (3\alpha_n + \beta_n)x_1 + 2\beta_n x_2 & -2\beta_n x_2 - 3\alpha_n x_1 & 0 & 0 \\ 0 & -2\beta_n x_2 - 3\alpha_n x_1 & 3\alpha_n x_1 + (2\alpha_n + 2\beta_n)x_2 + 3\beta_n x_3 & -3\beta_n x_3 - 2\alpha_n x_2 & 0 \\ 0 & 0 & -3\beta_n x_3 - 2\alpha_n x_2 & 2\alpha_n x_2 + (\alpha_n + 3\beta_n)x_3 + 4\beta_n x_4 & -4\beta_n x_4 - \alpha_n x_3 \\ 0 & 0 & 0 & -4\beta_n x_4 - \alpha_n x_3 & \alpha_n x_3 + 4\beta_n x_4 \end{bmatrix}$$

$$D_{Na} = \begin{bmatrix} d_1 & -3\alpha_m y_{00} - \beta_m y_{10} & 0 & 0 & -\alpha_h y_{00} - \beta_h y_{01} & 0 & 0 & 0 \\ -3\alpha_m y_{00} - \beta_m y_{10} & d_2 & -2\alpha_m y_{10} - 2\beta_m y_{20} & 0 & 0 & -\alpha_h y_{10} - \beta_h y_{11} & 0 & 0 \\ 0 & -2\alpha_m y_{10} - 2\beta_m y_{20} & d_3 & -\alpha_m y_{20} - 3\beta_m y_{30} & 0 & 0 & -\alpha_h y_{20} - \beta_h y_{21} & 0 \\ 0 & 0 & -\alpha_m y_{20} - 3\beta_m y_{30} & d_4 & 0 & 0 & 0 & -\alpha_h y_{30} - \beta_h y_{31} \\ -\alpha_h y_{00} - \beta_h y_{01} & 0 & 0 & 0 & d_5 & -3\alpha_m y_{01} - \beta_m y_{11} & 0 & 0 \\ 0 & -\alpha_h y_{10} - \beta_h y_{11} & 0 & 0 & -3\alpha_m y_{01} - \beta_m y_{11} & d_6 & -2\alpha_m y_{11} - 2\beta_m y_{21} & 0 \\ 0 & 0 & -\alpha_h y_{20} - \beta_h y_{21} & 0 & 0 & -2\alpha_m y_{11} - 2\beta_m y_{21} & d_7 & -\alpha_m y_{21} - 3\beta_m y_{31} \\ 0 & 0 & 0 & -\alpha_h y_{30} - \beta_h y_{31} & 0 & 0 & -\alpha_m y_{21} - 3\beta_m y_{31} & d_8 \end{bmatrix}$$

and with diagonal entries:

$$\begin{aligned} d_1 &= (3\alpha_m + \alpha_h)y_{00} + \beta_m y_{10} + \beta_h y_{01} \\ d_2 &= (\beta_m + 2\alpha_m)y_{10} + 2\beta_m y_{20} + 3\alpha_m y_{00} + \alpha_h y_{10} + \beta_h y_{11} \\ d_3 &= (2\beta_m + \alpha_m)y_{20} + 3\beta_m y_{30} + 2\alpha_m y_{10} + \alpha_h y_{20} + \beta_h y_{21} \\ d_4 &= 3\beta_m y_{30} + \alpha_m y_{20} + \alpha_h y_{30} + \beta_h y_{31} \\ d_5 &= 3\alpha_m y_{01} + \beta_m y_{y11} + \beta_h y_{01} + \alpha_h y_{00} \\ d_6 &= (\beta_m + 2\alpha_m)y_{11} + 2\beta_m y_{21} + 3\alpha_m y_{01} + \beta_h y_{11} + \alpha_h y_{10} \\ d_7 &= (2\beta_m + \alpha_m)y_{21} + 3\beta_m y_{31} + 2\alpha_m y_{11} + \beta_h y_{21} + \alpha_h y_{20} \\ d_8 &= 3\beta_m y_{31} + \alpha_m y_{21} + \beta_h y_{31} + \alpha_h y_{30} \end{aligned}$$

The vector $\mathbf{x}$ is composed of components $x_i (i = 0,1,2,3,4)$ representing the proportion of potassium channels with i open gates of type n. The entries of $\mathbf{y}$ are denoted as $y_{ij} (i = 0,1,2,3$ and $j = 0,1)$ representing the proportion of sodium channels with i open m subunits and j open subunits of type h. While Eqn. 2 is valid for a large number of channels, it has been shown to be a very accurate representation of the Markov chain model even for a small number of channels [14].

We are interested in a neural network in which the connections between neurons are unidirectional and the local dynamics are described by the Fox and Lu system size model (Eqn. 2). The I_{syn} term represents current input from the chemical synapses of other neurons in the network. Such a term is given by the following set of ordinary differential equations [7,4,16]:

$$\begin{aligned} I_{syn} &= \frac{(V_r - V_i)}{\omega} \sum_{j=1}^{N} \varepsilon_{ij} s_j \\ \dot{s}_i &= \frac{5(1 - s_i)}{1 + \exp(-\frac{V_i + 3}{8})} - s_i \end{aligned}$$

Here, V_r is the synaptic reversal potential set to $20mV$ [28], s_i is the post-synaptic potential, ε_{ij} represents the synaptic coupling strength between the j^{th} presynaptic neuron and the i^{th} postsynaptic neuron, and ω is the number of presynaptic connections. The remaining parameter, I_{inj}, determines whether or not action potentials occur [26]. For small values of $I_{inj}, (I_{inj} < 6.27\mu A/cm^2)$, the deterministic Hodgkin-Huxley model resides in a silent regime in that action potentials are not generated. When the injected current is greater

than $9.78\mu A/cm^2$, the deterministic Hodgkin-Huxley model enters the repetitive firing regime. Between these values, known as the excitable region, the model shows bistability between silence and repetitive firing.

In this paper, we are interested in how channel noise affects the synchronicity of neuron spiking at different firing rates. In order to quantitatively study neural synchronicity, we use the order parameter R defined as:

$$R(t) = \left| \frac{1}{N} \sum_{j=1}^{N} \exp(i\theta_j) \right| \tag{3}$$

where $\theta_j(t)$ is the phase of the jth neuron defined by $2\pi m + 2\pi \frac{t-t_{j,m}}{t_{j,m+1}-t_{j,m}}$ [2,4]. In this equation, $t_{j,m}$ denotes the time when neuron j emits spike m $(m = 0, 1\cdots)$. Eqn. 3 is designed in such a way that the first spike begins at $\theta = 0$ and the phase increases linearly until the next spike occurs at $\theta = 2\pi$. If all neurons are completely synchronized, then $\theta_1(t) = \cdots = \theta_N(t)$, and hence: $R = \left| \frac{1}{N} \sum_{j=1}^{N} \exp(i\theta_j) \right| = \left| \frac{1}{N} N \exp(i\theta_1) \right| = |\exp(i\theta_1)| = 1$. Therefore, R values are closer to unity when neurons have more synchronized spike times.

3 Results

All simulations were based on the system of stochastic differential equations Eq. 2. We used the Euler-Maruyama method [19,12] with time step $\Delta t = 10\mu s$. Unless noted otherwise, initially each neuron in the network was assumed to be in the resting state.

3.1 Frequency-Current Relationship

To understand how the number of channels affects the firing rate of a Hodgkin-Huxley neuron, we analyze the relationship between firing frequency of a stochastic neuron and the input current. In the squid axon modeled by Hodgkin and Huxley, the ratio of sodium channel density to potassium channel density is approximately $60\mu m^{-2}$: $18\mu m^{-2}$, and we use these values for our simulations [9]. Defining A to be the membrane area, the total number of sodium channels is given by $60 \times A$ and the total number of potassium channels is $18 \times A$. From Eqn. 2, the parameter A controls the magnitude of fluctuations from the channel noise as $A^{-1/2}$. Therefore, smaller channel area results in larger fluctuation magnitude whereas larger channel area results in smaller fluctuation magnitude. The resulting firing frequencies as a function of input current for different membrane areas are given in Figure 1.

The results show that in the absence of input current, the size of the channel area is what primarily determines the rate of spontaneous firing. As the input current increases, the firing rates for all different areas converge towards each other and the firing rate becomes independent of the channel area. With an increase in current, the neurons enter the repetitive firing regime so fluctuations in the membrane voltages should produce only minor changes in the frequency of spikes. Therefore, channel noise has a larger effect on the firing rate at low input currents.

3.2 Channel Number Effect on Synchronization

To understand how the number of channels affects the synchronicity of neurons, we consider a simple three member neural network with unidirectional excitatory connections and local dynamics given by Eqn 2. Such a system is shown in Figure 2. In this example, we assume the connections to have identical coupling constants $\varepsilon_{13} = \varepsilon_{21} = \varepsilon_{32} = 0.10$ and zero otherwise.

Because the neurons all start with the same initial condition, we have that $R(0) = 1$ regardless of the value of the channel area, i.e. all the neurons begin completely synchronized. However, as time passes, the degree of synchronization changes. Fig. 3 shows simulations of the three neuron neural network with varying channel area. Although the degree of synchronization for smaller area changes more rapidly than in the case of larger channel area, the degree of synchronization appears to reach the same steady state value and hover around this value. From this simulation, the channel area only affects the time to reach the steady state synchronization value but not the steady state synchronization value itself. Since changing channel area changes the firing rate (see Fig. 1), this suggests that there is an inverse relationship between the firing rate and time it takes to reach a steady state synchronization level (and consequently, a direct relationship between channel area and time to reach steady state.)

3.3 Derivation

In order to justify the behavior observed as channel noise changes in Fig. 3, let us consider a two neuron model. We will extend the result to a larger network afterwards. In large network modeling, the distribution of spike times is highly irregular, and modeling neurons in the network as a Poisson process is widely used [36,13,22]. As shown in Figure 1, for a given input current, channel noise affects the firing rate of a neuron. Therefore, we can understand the relationship between channel noise and synchronization by studying the relationship between synchronization and firing rate.

To understand why neurons in our network reach the same steady state synchronization level regardless of the channel area, our aim is to calculate the expectation of our order parameter $R(t)$, which we denote as $E[R(t)]$. Let us

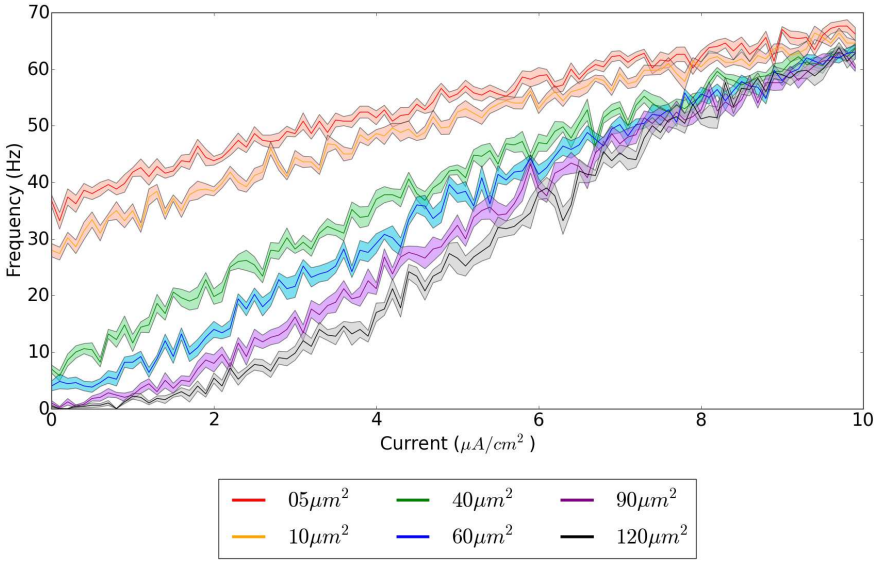

Fig. 1 Relationship between input current and firing frequency for varying membrane areas. Solid lines show the mean firing frequency averaged over 50 simulations. Shaded areas show one standard deviation of firing frequency from the mean.

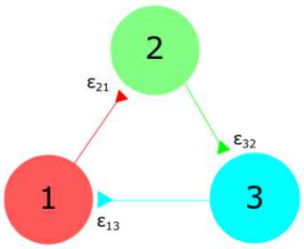

Fig. 2 Schematic drawing showing three unilaterally connected excitatory neurons with coupling strengths $\varepsilon_{13}, \varepsilon_{21}$, and ε_{32}

assume we have two neurons N_1 and N_2 whose spike times follow a Poisson distribution with rate parameter λ, and

$$E[R(t)] = E\left[\sqrt{R(t)^2}\right] = \frac{1}{2}E\left[\sqrt{|e^{i\theta_1(t)} + e^{i\theta_2(t)}|^2}\right]$$
$$= \frac{1}{2}E\left[\sqrt{2+2\cos(\theta_1(t) - \theta_2(t))}\right]$$

To compute this expectation, we are required to find the joint distribution of θ_1 and θ_2. When neurons are weakly coupled, we assume that we can approximate each one as essentially independent of the others, that is, that is, that we only need to find the density function of θ_1. We will later ascertain this assumption by comparing our theoretical results for independent neurons with numerical simulations for weakly coupled neurons.

From the definition of θ, only the random term $\frac{t-t_m}{t_{m+1}-t_m}$ has any bearing on the order parameter. Therefore to understand the distribution of θ, we only need to understand the distribution of $\frac{t-t_m}{t_{m+1}-t_m}$. Since we observe some steady state of synchronization in the simulations after time passes, consider a time t where t is large enough so that at least one spike has occurred before time t. Let X be a random variable describing the length of time between our time t and the time of the most recent spike before time t. Moreover, let Y be the length of time between time t and the next spike after time t. Notice that the ratio $\frac{X}{X+Y}$ corresponds directly with the $\frac{t-t_m}{t_{m+1}-t_m}$ term in the definition of θ. We need to add one constraint to X. Because X is the length of time between t and the previous spike, the maximum value X can take is t (otherwise a spike had to occur before time 0, which can not happen). Therefore, $\frac{t-t_m}{t_{m+1}-t_m}$ can be modeled by $\frac{\min\{X,t\}}{\min\{X,t\}+Y}$. Since the spike times of the neurons are being treated as Poisson processes, the wait time between spikes is an exponential distribution with rate parameter λ. Therefore, we have that Y has an exponential distribution with rate parameter λ, X also has an exponential distribution with rate parameter λ, and X and Y are independent of each other.

Let us employ a small trick to simplify matters. Exponential distributions have the scaling property, which means that if X has an exponential distribution with rate λ, then X has the same distribution as $\lambda^{-1}\xi$ where ξ is an exponential random variable with rate 1. Thus, Y also follows the distribution $\lambda^{-1}\eta$ where η is an exponential random variable with rate 1. Putting everything together, we have:

$$\frac{t-t_m}{t_{m+1}-t_m} \sim \frac{\min\{X,t\}}{\min\{X,t\}+Y} = \frac{\min\{\lambda^{-1}\xi,t\}}{\min\{\lambda^{-1}\xi,t\}+\lambda^{-1}\eta}$$
$$= \frac{\min\{\xi,\lambda t\}}{\min\{\xi,\lambda t\}+\eta}$$

Assuming λt is large enough, we can approximate the distribution of θ to be that of $\frac{\xi}{\xi+\eta}$ where ξ and η are inde-

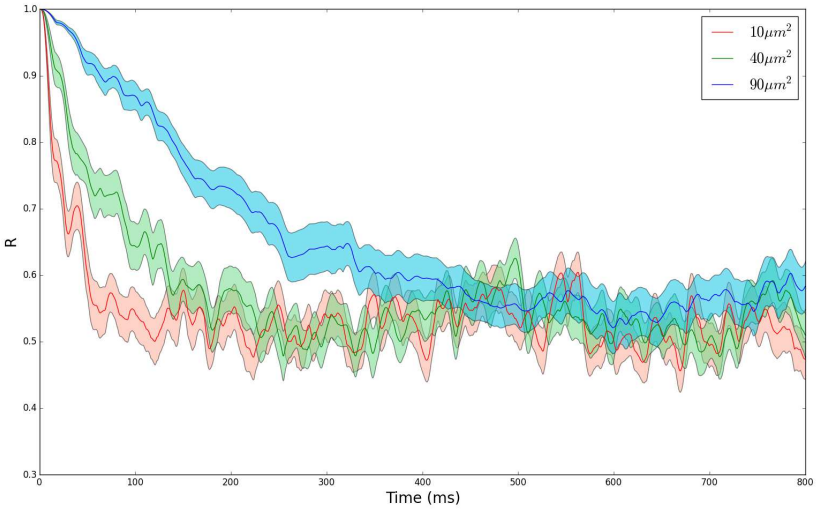

Fig. 3 Simulations of Eqn. 2 using the system shown in Fig. 2 for varying channel areas. Bold lines represent the mean after 50 simulations while shaded areas show one standard deviation from the mean. Injected current was $10.0\mu A/cm^2$.

pendent exponential random variables with rate parameter 1. To find the density function of θ, we only need to determine the density function for $\frac{\xi}{\xi+\eta}$. To calculate this density function, we will find the cumulative distribution function and take its derivative. Note that $0 < \frac{\xi}{\xi+\eta} < 1$, so let us pick an arbitrary $a \in (0,1)$ to use for calculating the distribution function. We use $f_\xi(x)$ to mean the density function of ξ in the derivation. We have:

$$\begin{aligned} P\left(\frac{\xi}{\xi+\eta} \leq a\right) &= P\left(\frac{\xi+\eta}{\xi} \geq \frac{1}{a}\right) \\ &= P\left(\eta \geq \xi\left(\frac{1}{a}-1\right)\right) \\ &= \int_0^\infty P\left(\eta \geq s\left(\frac{1}{a}-1\right)\right) f_\xi(s)ds \\ &= \int_0^\infty e^{-s\left(\frac{1}{a}-1\right)} e^{-s} ds \\ &= \int_0^\infty e^{-\frac{s}{a}} ds \\ &= a \end{aligned}$$

This means that $\frac{\xi}{\xi+\eta}$ has the exact same distribution as a uniform random variable on $(0,1)$. Consequently, the density function of θ is just 1. Returning to our calculation of the expectation of synchronization:

$$\begin{aligned} E[R(t)] &= \frac{1}{2}E\left[\sqrt{2+2\cos(\theta_1(t)-\theta_2(t))}\right] \\ &= \frac{1}{2}\int_0^1\int_0^1 \sqrt{2+2\cos(2\pi x_1 - 2\pi x_2)}dx_1 dx_2 \end{aligned} \quad (4)$$

This double integral can be solved exactly by utilizing a simple substitution and recognizing that we are integrating over one period of the cosine function,

$$\begin{aligned} E[R(t)] &= \frac{1}{2}\int_0^1\int_0^1 \sqrt{2+2\cos(2\pi x_1 - 2\pi x_2)}dx_1 dx_2 \\ &= \frac{1}{8\pi^2}\int_0^{2\pi}\int_0^{2\pi} \sqrt{2+2\cos(x_1 - x_2)}dx_1 dx_2 \\ &= \frac{1}{4\pi}\int_0^{2\pi} \sqrt{2+2\cos(x_1)}dx_1 \\ &= \frac{2}{\pi} \end{aligned}$$

Remarkably, we have shown that in the long-term limit of weakly coupled neurons, the expected steady state synchronization level has no dependence on the firing rate (membrane area) of the neurons and will confirm that, as already implicit, it only depends on the number of neurons in the network. In order to obtain a solution for the two-neural-network system, we needed to make a few assumptions: (a) the neurons in the network were weakly coupled to approximate them as independent of each other, and (b) the quantity λt is sufficiently large. Expanding on the second point, recall the we approximated $\min\{\xi, \lambda t\}$ by ξ. Since ξ is exponentially distributed with rate parameter 1, then $P(\xi \leq \lambda t) = 1 - \exp(-\lambda t)$. Because of the exponential decay dependence on λt, this means that λt does not have to be very large before one can approximate $\min\{\xi, \lambda t\}$ by ξ with high probability. With the application to neurons, this implies that when the firing rate of neurons is higher (small membrane area), we should expect less time to reach a steady state synchronization level. Conversely, with a lower firing rate (large

membrane area), we should expect a longer time to reach steady state synchronization. The high and low firing rates correspond with lower and higher channel noise magnitude respectively. Therefore, this derivation provides justification for the observation in Fig. 3 that larger channel noise magnitude in neurons results in faster synchronization.

To expand the result above to a larger neuron network, note that the only place where changes will occur is in the term under the radical. That term results from simplifying $\sqrt{R(t)^2}$, and a formula for $E[R(t)]$ as follows:

$$E[R(t)] = \frac{1}{N}\int_0^1 \sqrt{N + \sum_{\substack{j,k=1 \\ j\neq k}}^{N} \cos(2\pi x_j - 2\pi x_k)}\, dx_1 \ldots dx_N \tag{5}$$

Unlike the two neural network case, higher dimensional cases of Eqn. 5 must be evaluated numerically. Numerical estimations for the steady state synchronization predicted by Eqn. 5 for different numbers of neurons N can be found in Table 2

Table 2 Steady state synchronization values estimated from Monte Carlo simulations of Eqn. 5

Number of Neurons (N)	Steady State Synchronization Value
2	0.636
3	0.525
4	0.450

The comparison between the values obtained above and numerical simulations is shown in Fig. 4. As shown in Fig. 4, our estimation of the steady state synchronization values as determined by Eqn. 5 is quite accurate. For each of the neural network sizes, the synchronization value begins hovering around the steady state value after approximately 100 ms.

It is also worth noting that based on our results, the connectivity of neurons in the network has no bearing on the steady state synchronization as long as the coupling is weak. To emphasize, the importance of synchronization of the network is not on the connectivity of neurons, or the initial states of the neurons, but only in the number of neurons involved in the network. The role of noise is to help change the rate at which the network reaches a steady state synchronization level but does not change the level itself.

3.4 Large Membrane Area

In the derivation of our formula, we have approximated the spiking pattern as a Poisson distribution due to the irregularity of spike times in neural networks. One might expect that if the area of the neuron grows very large so that the magnitude of fluctuations is smaller and the dynamics of the stochastic model align very closely with the deterministic behavior, then the synchronization would not reach the steady state and instead retain a synchronization value close to 1 (i.e. completely synchronized). It feels as if one could ignore the fluctuations due to channel noise when the number of channels is extraordinarily large. Surprisingly, the answer to this is no. To examine this, we have considered an area of $300\mu m^2$ (equivalent to $18,000$ sodium channels and $5,400$ potassium channels) whose results are shown in Fig. 5.

Despite the similarity of the the stochastic and deterministic dynamics (Fig. 5), there are slight mismatches in spike timing due to the stochasticity of the Fox and Lu model. These slight mismatches accumulate over a lengthy period of time, and hence the order parameter decreases over time, albeit slowly. Even with the magnitude of the fluctuations from the channel noise being very small so that the spike timing is reasonably predictable, the degree of synchronization still decreases to the steady state value predicted by Eqn. 5. Our simulations and results suggest that channel noise should be accounted for in the modeling of real neuron synchronization regardless of the magnitude of fluctuations.

3.5 Expected Time to Reach Steady State

As we have shown, increasing channel area does not change the expected steady state synchronization value, but instead increases the time it takes to reach that value. Here, we would like to quantify this observation. In our simulations, once the synchronization level gets near the expected value we calculated in Eqn. 5, it hovers around that value. We consider the time to reach the steady state when our order parameter is within 0.02 of the value calculated by Eqn. 5. The results are shown in Fig. 6. Here we have considered the case of repetitive firing where we inject each neuron with a current of $10.0\mu A/cm^2$. As suggested by Fig. 6, there is a linear relationship between the membrane area and the expected time to synchronization. This also means that in the limit of infinitely many channels where the dynamics become identical to the Hodgkin-Huxley model, the time to reach the steady state synchronization is "infinite" in the sense that it never happens, which is in agreement with the order parameter of the Hodgkin Huxley never reaching a steady state value less than 1. However, as long as the number of channels is finite, Fig. 6 shows that the order parameter will eventually reach the expected steady state synchronization.

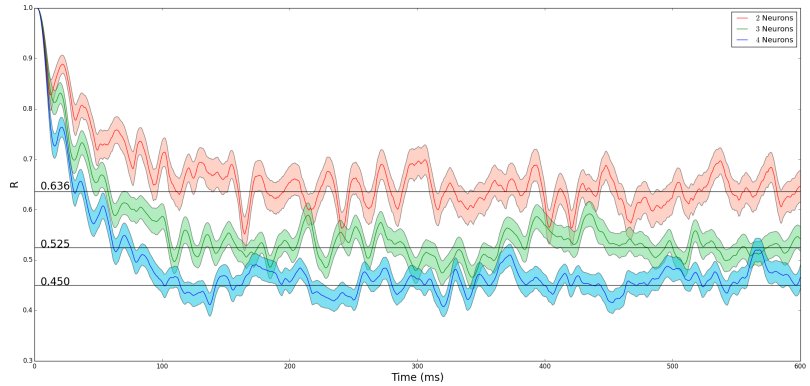

Fig. 4 Simulations showing synchronization parameter behavior for neuron networks of $2, 3$, and 4 neurons. Straight lines show estimated steady state synchronization values as determined by Eqn. 5. Each neuron in the network had an area of $40\mu m^2$ and an injected current of $8.0\mu A/cm^2$. Bold lines represent the mean after 100 simulations while shaded areas show one standard deviation from the mean.

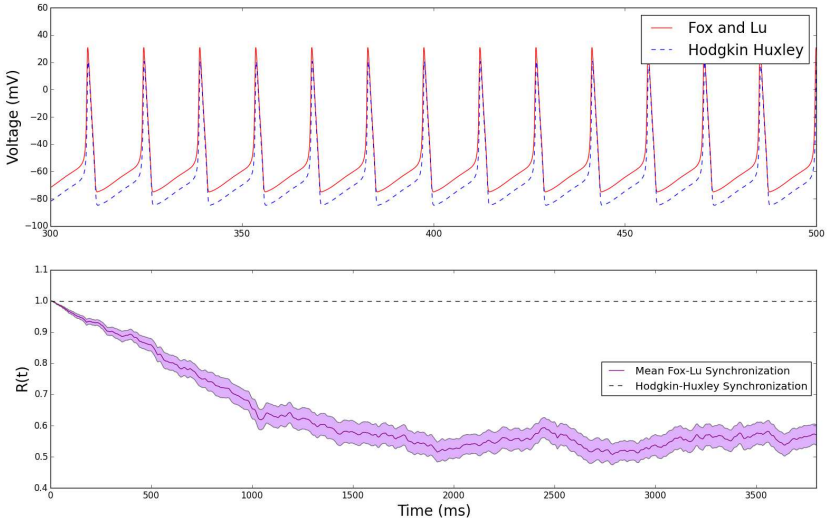

Fig. 5 (a) Comparison of membrane voltages for the deterministic Hodgkin-Huxley model and Fox and Lu model with membrane area of $300\mu m^2$. Both plots were conducted with input current of $10.0\mu A/cm^2$. Membrane voltage for the Hodgkin-Huxley model was offset by 10 mV for clarity. (b) Order parameter for the system shown in Fig. 2 where all three neurons are either deterministic or stochastic with an area of $300\mu m^2$. The bold line shows the mean order parameter value over 50 realizations, and the shaded area shows one standard deviation from the mean.

4 Conclusion

In this paper, we have sought to examine the effects of channel noise on neural network synchronization. Because real neurons have finitely many channels, the stochastic opening and closing of these channels leads to fluctuations in the membrane voltage that are not accounted for in the deterministic Hodgkin-Huxley model. In order to account for these fluctuations, we used the Fox and Lu system size expansion model because (a) it is a highly accurate approximation to the gold standard (but computationally expensive) Markov Chain model, and (b) it is a far more computationally efficient model than the Markov Chain model [10, 14].

We first looked at the relationship between firing frequency and input current in the presence of different magnitudes of channel noise. These simulations showed that channel noise had a larger effect on the firing rate in the absence of input current, but the effect was weakened as input current increased. We then looked at numerical simulations to qualitatively describe the effect of channel noise on neural network synchronization. We observed in Fig. 3 that (a) the neural networks hovered around a steady state synchronization level after some time, and (b) that increasing channel noise shortened the time it took to reach that synchronization level. In addition, we were able to derive a formula to accurately estimate the long term expected steady state syn-

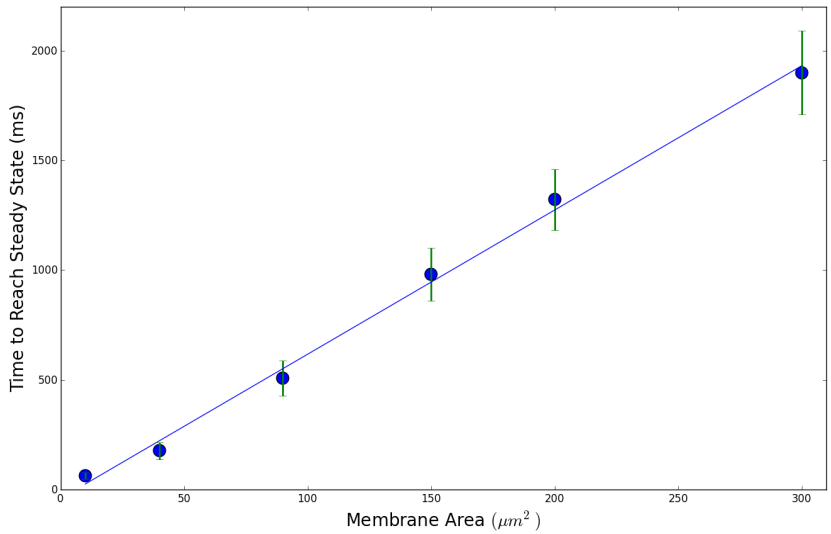

Fig. 6 Expected time (circles) for the mean order parameter to reach the steady state synchronization level. To calculate the expected time, we used the three neuron network in Fig. 2 with each neuron modeled by the Fox and Lu equations in Eqn. 2, injected each neuron with $10.0\mu A/cm^2$, and measured the time for the mean order parameter over 50 simulations to come within 0.02 of the expected steady state based on Eqn. 5. Vertical bars show 1 standard deviation from the mean.

chronization level. In the derivation of our formula, it was necessary to make a few assumptions. First, we needed to assume that the neurons were weakly coupled so that we can treat them as essentially independent from each other. In our simulations, we set the coupling constants $\varepsilon_{ij} = 0.1$, which is a biologically plausible value [17]. In addition, the derivation required λt to be large where λ is the firing rate. This requirement illustrates two features: that (a) as firing rate decreases (i.e. number of channels increases), the time to reach the steady state synchronization level increases, and (b) as firing rate increases, the steady state synchronization is reached faster. This observation was confirmed by the simulations shown in Fig. 3. Our work suggests that despite the randomness within the model, channel noise causes neural networks to reach a steady state level of synchronization provided they are weakly coupled, and the steady state value only depends on the number of neurons in the network as suggested by Fig. 4.

We then considered the network in Fig. 2 where the membrane area was very large for each neuron, and each neuron was in the repetitive firing regime. The purpose of doing this was to observe the synchronization behavior when the stochastic dynamics are very close to the deterministic dynamics. Even when the dynamics are extremely similar, the small amount of channel noise causes a big change in the degree of synchronization. While three coupled Hodgkin-Huxley neurons (without noise) remain completely synchronized, the small amount of channel noise causes them to desynchronize as observed in Fig. 5. The reason for this is that the small variation in the timing of the spikes causes the phases of the neurons to gradually drift apart

Finally, we showed that there seems to be an approximately linear relationship between the membrane area and the expected time to reach the steady state synchronization level. This result shows that in the limit of infinitely many channels, the steady state synchronization we expect to reach from Eqn. 5 is never reached. This is in agreement with the simulation shown in Fig. 5 where as the channel number grows to infinity, the stochastic dynamics converge to the deterministic dynamics, and the order parameter doesn't change for all time. However, for any finite number of channels, the simulation suggests that the expected steady state will be reached eventually. Ultimately, our paper strongly supports the notion that valuable insight can be gained by incorporating channel noise in the study of neural synchronization.

Acknowledgements We gratefully acknowledge support by the U. S. Office of Naval Research (ONR) under Grant No. N00014-13-1-0205. We also wish to acknowledge Patrick Fitzsimmons for his help in deriving a formula for the steady state synchronization level.

References

1. Abuhassan, K., Coyle, D., Maguire, L.: Compensating for thalamocortical synaptic loss in Alzheimer's disease. Frontiers in Computational Neuroscience **8** (2014)
2. Acebrón, J.A., Bonilla, L.L., Vicente, C.J.P., Ritort, F., Spigler, R.: The kuramoto model: A simple paradigm for synchronization phenomena. Reviews of modern physics **77**(1), 137 (2005)

3. Antzoulatos, E.G., Miller, E.K.: Increases in functional connectivity between prefrontal cortex and striatum during category learning. Neuron **83**(1), 216–225 (2014)
4. Borges, R., Borges, F., Lameu, E., Batista, A., Iarosz, K., Caldas, I., Viana, R., Sanjuán, M.: Effects of the spike timing-dependent plasticity on the synchronisation in a random hodgkin–huxley neuronal network. Communications in Nonlinear Science and Numerical Simulation **34**, 12–22 (2016)
5. Bukoski, A., Steyn-Ross, D., Steyn-Ross, M.L.: Channel-noise-induced critical slowing in the subthreshold hodgkin-huxley neuron. Physical Review E **91**(3), 032,708 (2015)
6. Buzsaki, G.: Rhythms of the Brain. Oxford University Press (2006)
7. Destexhe, A., Mainen, Z.F., Sejnowski, T.J.: An efficient method for computing synaptic conductances based on a kinetic model of receptor binding. Neural computation **6**(1), 14–18 (1994)
8. Fell, J., Axmacher, N.: The role of phase synchronization in memory processes. Nature reviews neuroscience **12**(2), 105–118 (2011)
9. Ferreira, H.G., Marshall, M.W.: The biophysical basis of excitability. Cambridge University Press (1985)
10. Fox, R.F., Lu, Y.n.: Emergent collective behavior in large numbers of globally coupled independently stochastic ion channels. Physical Review E **49**(4), 3421 (1994)
11. Fries, P.: A mechanism for cognitive dynamics: neuronal communication through neuronal coherence. Trends in cognitive sciences **9**(10), 474–480 (2005)
12. Gard, T.C.: Introduction to stochastic differential equations. M. Dekker (1988)
13. Gerstner, W., Kistler, W.M., Naud, R., Paninski, L.: Neuronal dynamics: From single neurons to networks and models of cognition. Cambridge University Press (2014)
14. Goldwyn, J.H., Imennov, N.S., Famulare, M., Shea-Brown, E.: Stochastic differential equation models for ion channel noise in hodgkin-huxley neurons. Physical Review E **83**(4), 041,908 (2011)
15. Goldwyn, J.H., Shea-Brown, E.: The what and where of adding channel noise to the hodgkin-huxley equations. PLoS Comput Biol **7**(11), e1002,247 (2011)
16. Golomb, D., Rinzel, J.: Dynamics of globally coupled inhibitory neurons with heterogeneity. Physical review E **48**(6), 4810 (1993)
17. Gray, E.: Electron microscopy of synaptic contacts on dendrite spines of the cerebral cortex. Nature **183**(4675), 1592–1593 (1959)
18. Hammond, C., Bergman, H., Brown, P.: Pathological synchronization in Parkinson's disease: networks, models and treatments. Trends in Neurosciences **30**(7), 357–364 (2007)
19. Higham, D.J.: An algorithmic introduction to numerical simulation of stochastic differential equations. SIAM review **43**(3), 525–546 (2001)
20. Hodgkin, A., Katz, B.: The effect of temperature on the electrical activity of the giant axon of the squid. The Journal of physiology **109**(1-2), 240–249 (1949)
21. Hodgkin, A.L., Huxley, A.F.: A quantitative description of membrane current and its application to conduction and excitation in nerve. The Journal of physiology **117**(4), 500 (1952)
22. Izhikevich, E.M.: Simple model of spiking neurons. IEEE Transactions on neural networks **14**(6), 1569–1572 (2003)
23. Izhikevich, E.M.: Which model to use for cortical spiking neurons? IEEE transactions on neural networks **15**(5), 1063–1070 (2004)
24. Jiruska, P., de Curtis, M., Jefferys, J.G., Schevon, C.A., Schiff, S.J., Schindler, K.: Synchronization and desynchronization in epilepsy: controversies and hypotheses. The Journal of physiology **591**(4), 787–797 (2013)
25. Lameu, E., Batista, C., Batista, A., Iarosz, K., Viana, R., Lopes, S., Kurths, J.: Suppression of bursting synchronization in clustered scale-free (rich-club) neuronal networks. Chaos: An Interdisciplinary Journal of Nonlinear Science **22**(4), 043,149 (2012)
26. Luccioli, S., Kreuz, T., Torcini, A.: Dynamical response of the hodgkin-huxley model in the high-input regime. Physical Review E **73**(4), 041,902 (2006)
27. Mino, H., Rubinstein, J.T., White, J.A.: Comparison of algorithms for the simulation of action potentials with stochastic sodium channels. Annals of biomedical engineering **30**(4), 578–587 (2002)
28. Popovych, O.V., Yanchuk, S., Tass, P.A.: Self-organized noise resistance of oscillatory neural networks with spike timing-dependent plasticity. Scientific reports **3**, 2926 (2013)
29. Schnitzler, A., Gross, J.: Normal and pathological oscillatory communication in the brain. Nature reviews neuroscience **6**(4), 285–296 (2005)
30. Singer, W.: Synchronization of cortical activity and its putative role in information processing and learning. Annual review of physiology **55**(1), 349–374 (1993)
31. Spencer, K.M., Nestor, P.G., Niznikiewicz, M.A., Salisbury, D.F., Shenton, M.E., McCarley, R.W.: Abnormal neural synchrony in schizophrenia. The Journal of Neuroscience **23**(19), 7407–7411 (2003)
32. Uhlhaas, P.J., Singer, W.: Neural synchrony in brain disorders: relevance for cognitive dysfunctions and pathophysiology. Neuron **52**(1), 155–168 (2006)
33. Uhlhaas, P.J., Singer, W.: Abnormal neural oscillations and synchrony in schizophrenia. Nature reviews neuroscience **11**(2), 100–113 (2010)
34. Wells, R.: Introduction to biological signal processing and computational neuroscience. an lcntr e-book. Moscow, ID: The University of Idaho (2007)
35. van Wijk, B., Beek, P.J., Daffertshofer, A.: Neural synchrony within the motor system: what have we learned so far? Frontiers in human neuroscience **6**, 252 (2012)
36. Zador, A.: When is an integrate-and-fire neuron like a poisson neuron? (1996)